Published in final edited form as:
Prostate. 2012 August 1; 72(11): 1214–1222. doi:10.1002/pros.22472.

Deficiency of DNA Repair Nuclease ERCC1-XPF Promotes Prostate Cancer Progression in a Tissue Recombination Model

Derek John Matoka[1], **Veronica Yao**[1], **Diana Sisca Harya**[1], **Jennifer Lien Gregg**[1], **Andria Rasile Robinson**[2], **Laura Jane Niedernhofer**[3], **Anil Parwani**[4], **Christoph Maier**[5], and **Dean John Bacich**[1]

[1]Department of Urology, University of Pittsburgh, Pittsburgh PA 15232

[2]Department of Human Genetics, University of Pittsburgh, Pittsburgh PA 15232

[3]Department of Microbiology and Molecular Biology, University of Pittsburgh, Pittsburgh, PA 15232

[4]Department of Pathology, University of Pittsburgh, Pittsburgh, PA 15232

[5]Department of Mathematics, Indiana University of Pennsylvania, Indiana PA 15705

Abstract

Background—The excision repair cross complementing (*ERCC1*) gene product plays a vital role in the nucleotide excision repair and DNA interstrand crosslink repair pathways, which protect the genome from mutations and chromosomal aberrations, respectively. Genetic deletion of *Ercc1* in the mouse causes dramatically accelerated aging. We examined the effect of *Ercc1* deletion in the development of prostate cancer in a prostate recapitulation model as *Ercc1* deficient mice die within four weeks of birth.

Methods—Prostate tissues from *Ercc1*$^{-/-}$ mice or wild-type littermates were combined with embryonic rat urogenital mesenchyme and grown as renal grafts for a total of 8, 16 and 24 weeks before histological, expression and proliferative evaluation.

Results—Invasive adenocarcinoma was observed in *Ercc1*$^{-/-}$ tissue recombinants but not wild-type as early as 8 weeks post-grafting. PIN-like lesions in *Ercc1*$^{-/-}$ tissue recombinants had more cytologic and architectural atypia than wild-type (p=0.02, p=0.0065 and p=0.0003 at the 8, 16 and 24 weeks respectively), as well as more proliferative cells (p=0.022 and p=0.033 at 8 and 16 weeks respectively). With serial grafting, *Ercc1*$^{-/-}$ tissue recombinants progressed to a more severe histopathological phenotype more rapidly than wild-type (p=0.011).

Conclusions—Results show that *ERCC1* and by implication the nucleotide excision repair and/or interstrand crosslink repair mechanisms protect against prostate carcinogenesis and mutations or polymorphisms affecting these DNA repair pathways may predispose prostate epithelial cells to transformation.

Keywords

ERCC1-XPF; nucleotide excision repair; interstrand crosslink repair; recombinant

Corresponding Author and Request for Reprints: Dr. Dean J Bacich, Ph.D., UPMC Shadyside, Department of Urology, 5200 Centre Avenue, Suite G-32, Pittsburgh PA 15232 USA, Phone: (412) 623-3913, Fax: (412) 623-3907, bacichdj@upmc.edu.

Disclosure Statement: The authors declare that they have no affiliations with any organization that may have a direct interest in the research described, or a real or perceived conflict of interest. The funders had no role in study design, data collection and analysis, decision to publish, or preparation of the manuscript.

Introduction

Prostate cancer is a serious threat to American men with 217,730 new diagnoses and 32,050 associated deaths estimated in 2010 (1). The exact etiology of prostate cancer is unknown, but evidence suggests that a decrease in DNA repair capacity may contribute to the development of this disease (2). Prostate carcinogenesis is a multistep process in which the accumulation of genetic alterations is postulated to promote the progression from normal prostate epithelium to invasive adenocarcinoma (3, 4). Inherited and highly penetrant germline mutations in DNA-damage response genes account for approximately 10% of all prostate cancers (4). However, the greater majority of prostate cancer is likely related to low penetrant germline mutations, an accumulation of somatic mutations, gene deletions and amplifications, chromosomal rearrangements, and changes in DNA methylation. The incidence of many of these genetic alterations may be significantly affected by common single nucleotide polymorphisms (SNPs) in DNA repair genes (4–8). A cell's diminished ability to repair DNA damage may result in oncogene activation and tumor suppressor inactivation. Indeed, reduced DNA repair capability significantly contributes to genetic instability and contributes to a number of solid tumors (9, 10). Although studies have shown an association between prostate cancer risk and germline mutations and SNPs in DNA repair genes (4–8), this relationship requires further elucidation.

The nucleotide excision repair (NER) pathway, removes helix-distorting DNA lesions from the genome (11). Over 40 genes, with 200 identified SNPs, are required for NER (12). Defects in NER are associated with increased prostate cancer risk (13, 14). Several common prostate cancer carcinogens, such as tobacco-related polycyclic aromatic hydrocarbons, heterocyclic aromatic amines and pesticides, produce DNA damage repaired by NER (15). Hu and colleagues found that lymphocytes from prostate cancer patients had a statistically significant lower NER capacity as compared to controls (14). Recently, Woelfeschneider *et al.*, demonstrated that a distinct *ERCC1* haplotype is associated with lower *ERCC1* mRNA expression in prostate cancer patients (16).

ERCC1 is required to bind and stabilize XPF *in vivo* to form a structure-specific endonuclease complex that incises the damaged strand of DNA 5′ to the lesion in NER (17). ERCC1-XPF is also required for the repair of DNA interstrand crosslinks and facilitates the repair of DNA double-strand breaks (18, 19). Mutations in *XPF* causes xeroderma pigmentosum characterized by photosensitivity and increased risk of skin cancer due to failure to repair UV-induced DNA damage (20). However, mutations that severely effect *XPF* expression lead to a progeroid syndrome (21). Deletion of *Ercc1*, the obligate binding partner of XPF, in the mouse also causes accelerated aging (21). The symptoms, histopathology, and metabolic, endocrine and gene expression changes observed in ERCC1$^{-/-}$ parallel those seen in natural aging. As prostate cancer incidence is highly correlated with age (1), models of early aging may offer insight into the etiology of prostate cancer. However, the short life span of *Ercc1*$^{-/-}$ mice (4 weeks) (21, 22) prevents the study of prostate cancer. To solve this problem, we used the tissue recombination model to examine the potential roles of Ercc1-XPF and NER in prostate cancer.

The tissue recombination model, which was first described by Cunha and colleagues (23), uses rat urogenital mesenchyme (rUGM) to induce embryonic and adult prostate epithelial cell growth, ductal branching morphogenesis and cytodifferentiation (24). Embryonic prostatic rudiments and adult prostates grafted under the renal capsule proliferate, undergo prostatic morphogenesis, and produce prostatic secretory proteins (24, 25). As this model can rescue prostatic rudiments, it can be used to investigate the role of genes in embryonic lethal animal models or animal models with a short-life span. Wang and colleagues used the tissue recombination model to rescue prostates from embryonically lethal *Rb*$^{-/-}$ mice and to

evaluate the effect of *Rb* deletion on prostate tissue (26). To achieve prostatic carcinogenesis in a timely fashion, tissue recombinants are treated with hormones (testosterone and 17β-estradiol, T&E2) at pharmacological doses. Using this hormone-induced tissue recombinant model, we discovered that ERCC1-XPF protects against rapid development of invasive prostatic adenocarcinoma.

Methods

Rescue of ERCC1 Prostatic Tissue

Ercc1$^{-/-}$ male mice and wild-type siblings were bred and genotyped as previously described (21). Prostates were harvested from euthanized 17–21 day-old mice. All animals were housed in the University of Pittsburgh Cancer Institute animal care facility, provided with food and drinking water *ad libitum* under controlled lighting conditions. and treated in accordance with approved IACUC protocols. The protocol was approved by the Institutional Animal Care and Use Committee at the University of Pittsburgh (Protocol number 0610805). All surgery was performed using Ketamine/Xylazine as an anesthesia, and all efforts were made to minimize suffering.

Tissue Preparation and Recombination

Rat urogential sinuses were removed from 18-day old embryonic fetuses of pregnant Sprague Dawley rats (Taconic) and separated into epithelial and mesenchyme components as previously described (27). Urogenital sinuses were digested with 10 mg/mL trypsin (Sigma Aldrich, St. Louis, MO) for 75 min at 4°C prior to mechanical separation of epithelial and mesenchymal components then the mesenchymal cells digested with 187 U/mL collagenase (Gibco) for 90 min at 37°C to obtain single-cells. Prostatic tissue from *Ercc1*$^{-/-}$ mice or wild-type littermates were combined with 250,000 rUGM cells in Type I rat tail collagen (BD) and setting solution (EBSS, $NaHCO_3$, 50mM NaOH). Tissue recombinants were incubated overnight at 37°C in RPMI-1640 supplemented with 10^{-8}M testosterone (Sigma Aldrich).

Sub-Capsular Renal Grafting and Induction of Carcinogenesis

Tissue recombinants were grown as subcapsular renal grafts in athymic mouse hosts (Nu/Nu CD1 mice). At the time of grafting, silastic capsules (1.54 mm inside diameter and 3.18 mm outside diameter (Dow-Corning Co.)) containing 25 mg of testosterone and 2.5 mg of 17β-estradiol were surgically implanted under the dermis. A recombinant consisting only of rUGM was grafted to ensure that the mesenchymal cells were not contaminated with rat epithelial cells.

Host animals were sacrificed at 8 weeks following grafting and tissue recombinants were carefully dissected from the host kidney. A portion of each tissue recombinant was fixed in 10% neutral buffered formalin and embedded in paraffin. The remaining portion of the tissue recombinant was recombined with fresh rUGM and grafted under the renal capsule of an athymic mouse implanted with fresh T&E2. After a total of 16 weeks, tissue recombinants were harvested for analysis, recombined with fresh rUGM, and regrafted under the renal capsule for a total of 24 weeks. Thus, tissue recombinants were grown in host mice for a total of 8, 16 and 24 weeks.

Histopathology

Tissue sections stained with Hematoxylin and Eosin (H&E) for histopathology; and Hoechst dye 33258 (Calbiochem) to confirm that the epithelium was of mouse origin and the stroma of rat origin (28). H&E, CK14 and p63 stained slides were blindly scored by a pathologist

for the presence of normal glands, hyperplasia, Prostatic Intraepithelial Neoplasia (PIN)-like lesions and lesions consistent with adenocarcinoma.

PIN-like lesions were scored as 1+, 2+ or 3+ indicating increasing architectural and cytological atypia (28; see supplementary data for features typical of each PIN score). PIN-like lesions scored 1+ (least severe) displayed prostatic hyperplasia with the glandular epithelial cells demonstrating uniform oval nuclei, which may be enlarged and/or exhibit weak hyperchromasia, and absent or inconspicuous nucleoli. PIN-like lesions scored 2+ (moderately severe) consisted of hyperplastic glands with larger cells, a higher nucleus to cytoplasmic ratio and more pronounced hyperchromasia. Nucleoli were more prominent and cells displayed predominately papillary type architecture with more crowding and stratification. A tufted type of architecture was occasionally observed. In order to obtain a score of 3+ (most severe), PIN-like lesions had a pronounced increase in cell size, increased pleomorphism, and striking hyperchromasia with enlarged nucleoli. Some cells had more than one nucleolus, a feature more commonly seen in neoplasia. Additionally, significant architectural disorder with the presence of papillary tufting was a characteristic of 3+ PIN. At low power, these foci were very prominent due to the consistent dark, hyperchromatic appearance of the nuclei that was in stark contrast to adjacent benign glands. There was also significant stratification of the nuclei which gave the appearance of multi-layering. In reviewing tissue recombinants, each recombinant was scored according to the most severe histopathology. For example, a tissue recombinant that exhibited a spectrum of 1+-3+ PIN-like lesions was considered to be 3+ PIN for the purpose of data analysis.

Immunohistochemistry

Tissue sections were stained using the Vector® M.O.M™ Peroxidase Kit (Vector Laboratories). Non-immune mouse IgG alone served as the control. Primary antibodies included: CK-14 (basal cells, AbCam); p63 (basal cells, NeoMarkers); and Ki-67 (proliferation, Fitzgerald Industries). Sections were developed using Nova Red solution (Vector Laboratories).

Proliferation Index

Proliferation index was compiled by manually counting epithelial nuclei staining positively with Ki-67 antibodies, and dividing this by the total number of epithelial cells observed in two microscopic fields from 6–15 tissue samples.

Anchorage-Independent Growth

A tissue recombinant (20mg) that had been grafted under the kidney capsule for 24 weeks were digested with 108U collagenase for at least 4 hours at 37°C and seeded in 6-well plates in a double layer agar culture system. The underlay contained culture media with a final agar concentration of 0.6% (Difco Laboratories) and the overlay contained culture media with a final agar concentration of 0.3%. The dishes were incubated at 37°C in a humidified atmosphere and photomicrographs were captured on a Nikon T1-SM microscope.

Statistical Analysis

Statistical analysis on proliferation index of the tissue recombinants was performed using the Student's *t-test*. Wilcoxon-Mann-Whitney test was used to analyze the incidence of PIN 1+, 2+ and 3+ in wild-type and *Ercc1*$^{-/-}$ tissue recombinants. The Fisher's exact test was used to analyze the incidence of PIN and foci with features of adenocarcinoma. The Jonckheere-Terpstra test was used to determine whether there was histopathological progression with serial grafting of the tissue recombinants.

Results

To evaluate the functional significance of ERCC1-XPF in prostate cancer, tissue recombinants consisting of prostate tissues from *Ercc1*$^{-/-}$ mice, which are also missing XPF (21), or prostate tissues from wild-type littermates and rUGM were compared at 8, 16 and 24 weeks post-implantation. H&E and p63-stained tissue recombinants were examined blindly by a genitourinary pathologist (Dr. Parwani) to determine the incidence of normal, hyperplasia, PIN-like lesions and carcinoma.

The majority (7 of 11, 64%) of wild-type tissue recombinants consisted of either normal prostatic glands lined by columnar luminal epithelial cells (2 of 11, 18%) or focal hyperplastic glands (5 of 11, 46%) (Table 1, Figure 1B). Hyperplastic glands exhibited multiple layers of polarized luminal epithelial cells. Some hyperplastic glands also displayed papillary projections. Only a third (4 of 11, 36%) of the wild-type tissue recombinants had 1+ or 2+ PIN-like lesions (Table 2, Figure 2). In contrast, the majority (13 of 18, 72%) of the *Ercc1*$^{-/-}$ tissue recombinants exhibited PIN-like lesions at 8 weeks (Table 1). Approximately 15% (2 of 13) of these PIN-like lesions were scored as 3+, a score that was absent in the wild-type recombinants (Table 2, Figure 2). Importantly, glands with features of cancer; characterized by nuclear pleomorphism, elevated epithelial proliferation, increased mitosis, and loss of basal epithelial cells, were observed in *Ercc1*$^{-/-}$ tissue recombinants (Figure 1C, D). *Ercc1*$^{-/-}$ tissue recombinants also had a significantly higher proliferation index than wild-type (p=0.022) (Figure 3B). In total, at the 8-week time point, *Ercc1*$^{-/-}$ tissue recombinants had a statistically worse pathology than wild-type tissue recombinants (p=0.020).

The number of wild-type tissue recombinants with PIN-like lesions increased from approximately 36% (4 of 11) at 8 weeks to 67% (10 of 15) at 16 weeks (Table 1). None of the wild-type tissue recombinants displayed 3+ PIN-like lesions or cancer even by 16 weeks (Table 2). In contrast, 100% of *Ercc1*$^{-/-}$ tissue recombinants exhibited either PIN-like lesions or glands with features of adenocarcinoma (Table 1 and Figure 2). Approximately 33% (5 of 15) of PIN-like lesions in *Ercc1*$^{-/-}$ tissue recombinants at 16 weeks were scored 3+ (Table 2), more than double the frequency at 8 weeks. These 3+ PIN-like lesions displayed hyperplasia, nuclear stratification, elevated nuclear to cytoplasmic ratio, papillary tufting, and disrupted basal cell layer (Figure 4A). In addition, about 12.5% (2 of 16) of the *Ercc1*$^{-/-}$ tissue recombinants displayed atypical glands that lacked basal cells (Table 1, Figure 2). Carcinoma was observed in the form of multiple, small, crowded glands with nuclear pleomorphism, elevated nuclear to cytoplasmic ratio, and abnormal mitosis (Figure 4A). The adjacent stroma and normal appearing glands were encroached upon by the invasive lesions. These *Ercc1*$^{-/-}$ tissue recombinants also showed a significantly higher proliferation index than wild-type tissue recombinants (p=0.033) (Figure 3). The histopathology of *Ercc1*$^{-/-}$ tissue recombinants was significantly worse than wild-type tissue recombinants at 16 weeks (p=0.0065).

At 24 weeks, approximately 82% (14 of 17) of wild-type tissue recombinants displayed PIN-like lesions (Table 1, Figure 2), reflecting a 15% increase from 16 weeks. In contrast, all of the *Ercc1*$^{-/-}$ tissue recombinants had PIN-like lesions or multiple small crowded glands with large pleomorphic nucleus, abnormal mitosis and prominent nucleoli (Table 1, Figure 4B). None of the wild-type tissue recombinants displayed 3+ PIN-like lesions or carcinoma even at 24 weeks, whereas 21% (3 of 14) of the ERCC1$^{-/-}$ tissue recombinants were scored as 3+ PIN (Table 2). Although the proliferation index of *Ercc1*$^{-/-}$ tissue recombinants was higher than wild-type, this did not reach statistical significance (p=0.195) at 24 weeks (Figure 3B). However, *Ercc1*$^{-/-}$ tissue recombinants displayed significantly worse histopathology relative to wild-type at 24 weeks (p=0.0003). Serial grafting led to

progressive derangement of prostatic architecture only in *Ercc1*$^{-/-}$ tissue recombinants as evidenced by a significant increase in the number of recombinants that displayed glands with features of adenocarcinoma (p=0.0110) (Table 1). When tissue recombinants composing of either *Ercc1*$^{-/-}$ or wild-type prostate tissues were digested and grown in semisolid medium, only cells from *Ercc1*$^{-/-}$ tissue recombinants were able to form colonies (Figure 5).

Conclusions

Considerable resources have been devoted to defining the underlying etiology and associated pathophysiology of prostate cancer, a disease that continues to be the second leading cause of cancer-related deaths in American men (1). Despite these efforts, a thorough understanding of the etiology of this disease remains elusive. Prostate cancer is a disease where incidence increases with age (1). As with other solid tumors, accumulation of DNA damage and genetic mutations with age promotes prostate cancer. Lockett and colleagues reported a significant association between reduced NER capacity and prostate cancer risk (13). This NER capacity correlates with *ERCC1* mRNA levels (29). Reduced DNA repair capacity may constitute a risk factor for cancer development (30). Suboptimal DNA repair in normal tissue leads to genomic instability, a critical step in carcinogenesis.

Utilizing the tissue recombination model first described by Cunha and colleagues (23), we evaluated the role that ERCC1-XPF DNA repair endonuclease contributes to prostate cancer. This was accomplished by rescuing prostatic tissues from progeroid *Ercc1*$^{-/-}$ mice at 2–3 weeks of life, and combining these tissues with rUGM. The pathology of the tissue recombinants were compared to those consisting of prostate tissues from wild-type sibling mice. This model provides an opportunity to follow the consequences of this isolated genetic deficiency over time. Tissue recombinants of both groups were exposed to pharmacological doses of T&E2 in order to reduce the long latent period typically associated with the development of an invasive tumor.

Ercc1$^{-/-}$ tissue recombinants demonstrated a more severe histopatholigical phenotype than their wild-type counterparts at each time point. Focal lesions demonstrating overcrowding of small glands, nuclear pleomorphism, increased nuclear to cytoplasmic ratio, increased mitosis, and a lack of CK-14/p63-positive basal cells were seen in the *Ercc1*$^{-/-}$ tissue recombinants by 8 weeks of growth under the renal capsule. These characteristics are consistent with invasive adenocarcinoma, and were not seen in wild-type tissue recombinants even at 24 weeks. The most severe histopathological feature observed in wild-type tissue recombinants was 2+ PIN-like lesions.

Increased mitosis in *Ercc1*$^{-/-}$ tissue recombinants was most apparent in epithelial cells of glands with features of carcinoma. This is accompanied by a significantly higher proliferation index, as measured by Ki-67 immunostaining, in *Ercc1*$^{-/-}$ compared to wild-type tissue recombinants at 8 (p=0.022) and 16 (p=0.033) weeks. However, the increased proliferation index in *Ercc1*$^{-/-}$ than in wild-type tissue recombinants at 24 weeks did not reach statistical significance (p=0.195) despite the presence of mitotic bodies in these tissues. This may be due to decreased proliferative capacity of the prostate tissues with serial grafting.

There were progressive tissue architectural and cytological abnormalities with serial grafting in *Ercc1*$^{-/-}$ tissue recombinants including loss of epithelial polarity, epithelial crowding, stratification and invasiveness. The number of *Ercc1*$^{-/-}$ tissue recombinants with invasive adenocarcinoma increased with serial grafting from 6% (1 of 18) at 8 weeks to approximately 18% (3 of 17) at 24 weeks, which was statistically significant (p=0.01). Our

results indicate that these atypical glands with features of invasive adenocarcinoma are transplantable and suggest that *Ercc1*$^{-/-}$ can undergo progressively severe histopathological alterations with serial grafting. Similarly, Wang and colleagues found that carcinoma observed in *Rb*$^{-/-}$ mice treated with hormones were transplantable when serially grafted to new hosts (26). The fact that we were able to grow these small atypical cells in semisolid medium (anchorage-independent growth) provides further evidence of their tumorigenicity.

Although both *Ercc1*$^{-/-}$ and wild-type tissue recombinants displayed PIN-like lesions, only *Ercc1*$^{-/-}$ tissue recombinants were scored 3+ (most severe) in cytological and architectural atypia. The presence of PIN-like lesions in wild-type tissue recombinants was consistent with exposure to T&E2 at pharmacological doses (26, 28). Wang and colleagues observed glands with cibriform pattern, which we classified as PIN, in *Rb*$^{+/+}$ prostatic recombinants treated with T&E2 (26). The wild-type tissue recombinants, therefore, provided a good control for histological changes caused by T&E2 administration. Therefore, all of the differences observed between *Ercc1*$^{-/-}$ and wild-type tissue recombinants are a direct consequence of reduced DNA repair of endogenous DNA damage, and indicates that reduced DNA repair capacity can promote hormonal prostate carcinogenesis.

ERCC1 expression was significantly down regulated in metastatic prostate cancer samples in a gene array study by Varambally et al.,(31) and was associated with the outlier group of metastatic samples with a COPA score of −4.962 (Oncomine 4.4). Glinsky et al.,(32) examine the expression status of 79 prostate cancer samples using expression arrays and revealed that ERCC1 expression was significantly down regulated in an outlier population of samples with positive surgical margins (COPA score −3.626). Vanaja et. al.,(33) demonstrated that ERCC1 expression is significantly down regulated specifically in prostate samples with a Gleason score of 9 in an outlier analysis of 32 prostate adenocarcinomas and 8 normal prostate, (COPA score −1.351). These above associations of ERCC1 down regulation with factors considered to be indicative of aggressive disease indicates that ERCC1 and its associated DNA damage repair pathways are likely critical modulators in prostate cancer progression in a subset of prostate cancer patients.

Our results indicate that ERCC1-XPF dependent DNA repair is critical for protecting prostate epithelial from transformation. This could be due to reduced capacity for repair of interstrand crosslinks, double-strand breaks or helix-distorting DNA lesions. Regardless, expression of ERCC1-XPF in individuals might serve as a good biomarker of prostate cancer risk. Many cancer therapeutics induce DNA damage that is repaired through mechanisms that require ERCC-XPF nuclease activity, including crosslinking agents and ionizing radiation. Thus, reduced expression of ERCC1-XPF may also serve as a good prognosticator of a patient’s likelihood of responding to specific cancer therapeutics.

Supplementary Material

Refer to Web version on PubMed Central for supplementary material.

Acknowledgments

Funding sources: D.J.M, V.Y, D.S.H and D.J.B Department of Urology, University of Pittsburgh; D.J.B. (CA138444) and A.R.R. and L.J.N. NCI (CA111525)

References

1. Jemal A, Siegel R, Xu J, Ward E. Cancer Statistics, 2010. CA Cancer J Clin. 2010; 60:277–300. [PubMed: 20610543]

2. Malins DC, Johnson PM, Wheeler TM, Barker EA, Polissar NL, Vinson MA. Age-related radical-induced DNA damage is linked to prostate cancer. Cancer Res. 2001; 61:6025–6028. [PubMed: 11507046]
3. Isaacs WB, Bova GS, Morton RA, Bussemakers MJ, Brooks JD, Ewing CM. Molecular biology of prostate cancer. Semin Oncol. 1994; 21:514–521. [PubMed: 7939745]
4. Coughlin SS, Hall IJ. A review of genetic polymorphisms and prostate cancer risk. Ann Epidemiol. 2002; 12:182–196. [PubMed: 11897176]
5. Dong JT. Prevalent mutations in prostate cancer. J Cell Biochem. 2006; 97:433–447. [PubMed: 16267836]
6. Damaraju S, Murray D, Dufour J, Carandang D, Myrehaug S, Fallone G, Field C, Greiner R, Hanson J, Cass CE. Parliament M. Association of DNA repair and steroid metabolism gene polymorphism with clinical late toxicity in patients treated with conformal radiotherapy for prostate cancer. Clin Cancer Res. 2006; 12:2545–2554. [PubMed: 16638864]
7. Johansson M, Van Guelpen B, Hultdin J, Wiklund F, Adami HO, Bälter K, Grönberg H, Stattin P. The MTHFR 667C → T polymorphism and risk of prostate cancer: results from the CAPS study. Cancer Causes Control. 2007; 18:1169–1174. [PubMed: 17846906]
8. Hooker S, Bonilla C, Akereyeni F, Ahaghotu C, Kittles RA. NAT2 and NER genetic variants and sporadic prostate cancer susceptibility in African Americans. Prostate Cancer Prostatic Dis. 2008; 11:349–356. [PubMed: 18026184]
9. Takebayashi Y, Nakayama K, Kanzaki A, Miyashita H, Ogura O, Mori S, Mutoh M, Miyazaki K, Fukumoto M, Pommier Y. Loss of heterozygosity of nucleotide excision repair factors in sporadic ovarian, colon and lung carcinomas: implication for their roles of carcinogenesis in human solid tumors. Cancer Lett. 2001; 174:115–125. [PubMed: 11689286]
10. Rockwell S, Yuan J, Peretz S, Glazer PM. Genomic instability in cancer. Novartis Found Sump. 2001; 240:133–142.
11. Sancar A, Tang MS. Nucleotide excision repair. Photochem Photobiol. 2003; 57:905–921. [PubMed: 8393197]
12. Wood RD, Mitchell M, Sgouros J, Lindahl T. Human DNA repair genes. Science. 2001; 291:1284–1289. [PubMed: 11181991]
13. Lockett KL, Snowhite IV, Hu JS. Nucleotide excision repair and prostate cancer risk. Cancer Lett. 2005; 220:125–135. [PubMed: 15766587]
14. Hu JJ, Hall MC, Grossman L, Hedayati M, McCullough DL, Lohman K. Case LD Deficient nucleotide repair capacity enhances human prostate cancer risk. Cancer Res. 2004; 64:1197–1201. [PubMed: 14871857]
15. Martin FL, Cole KJ, Muir GH, Kooiman GG, Williams JA, Sherwood RA, Grover PL, Phillips DH. Primary cultures of prostate cells and their ability to activate carcinogens. Prostate Cancer Prostatic Dis. 2002; 61:6470–6474.
16. Woelfelschneider A, Popanda O, Lilla C, Linseisen J, Mayer C, Celebi O, Debus J, Bartsch H, Chang-Claude J, Schmezer P. A distinct ERCC1 haplotype is associated with mRNA expression levels in prostate cancer patients. Carcinogenesis. 2008; 29:1758–1764. [PubMed: 18332046]
17. Gossage L, Madhusudan S. Current status of excision repair cross complementing-group 1 (ERCC1) in cancer. Cancer Treatment Reviews. 2007; 33:565–577. [PubMed: 17707593]
18. Niedernhofer LJ, Odijk H, Budzowska M, van Drunen E, Maas A, Theil AF, de Wit J, Jaspers NG, Beverloo HB, Hoeijmakers JH, Kanaar R. The structure-specific endonuclease ERCC1-XPF is required to resolve DNA interstrand cross-link-induced double-strand breaks. Mol Cell Biol. 2004; 24:5776–5787. [PubMed: 15199134]
19. Ahmad A, Robinson AR, Duensing A, van Drunen E, Beverloo HB, Weisberg DB, Hasty P, Hoeijmakers JH, Niedernhofer LJ. ERCC1-XPF endonuclease facilitates DNA double-strand break repair. Mol Cell Biol. 2008; 28:5082–5092. [PubMed: 18541667]
20. Sijbers AM, de Laat WL, Ariza RR, Biggerstaff M, Wei YF, Moggs JG, Carter KC, Shell BK, Evans E, de Jong MC, Rademakers S, de Rooij J, Jaspers NG, Hoeijmakers JH, Wood RD. Xeroderma pigmentosum group F causes by a defect in a structure-specific DNA repair endonuclease. Cell. 1996; 86:811–822. [PubMed: 8797827]

21. Niedernhofer LJ, Garinis GA, Raams A, Lalai AS, Robinson AR, Appeldoorn E, Odijk H, Oostendorp R, Ahmad A, van Leeuwen W, Theil AF, Vermeulen W, van der Horst GT, Meinecke P, Kleijer WJ, Vijg J, Jaspers NG, Hoeijmakers JH. A new progeroid syndrome reveals that genotoxic stress suppresses the somatotroph axis. Nature. 2006; 444:1015–1017. [PubMed: 17183304]
22. McWhir J, Selfridge J, Harrison DJ, Squires S, Melton DW. Mice with DNA repair gene (ERCC-1) deficiency have elevated levels of p53, liver nuclear abnormalities and die before weaning. Nat Genet. 1993; 5:217–224. [PubMed: 8275084]
23. Cunha GR, Sekkingstad M, Meloy BA. Heterospecific induction of prostatic development in tissue recombinants prepared with mouse, rat, rabbit and human tissues. Differentiation. 1983; 24:174–180. [PubMed: 6884617]
24. Hayashi N, Cunha GR, Parker M. Permissive and instructive induction of adult rodent prostatic epithelium by heterotypic urogenital sinus mesenchyme. Epithelial Cell Biol. 1993; 2:66–78. [PubMed: 8353595]
25. Cunha GR. Age-dependent loss of sensitivity of female urogenital sinus to androgenic conditions as a function of the epithelial-stromal interaction. Endocrinology. 1975; 95:665–673. [PubMed: 1175513]
26. Wang Y, Hayward SW, Donjacour AA, Young P, Jacks T, Sage J, Dahiya R, Cardiff RD, Day ML, Cunha GR. Sex hormone-induced carcinogenesis in Rb-deficient prostate tissue. Cancer Res. 2000; 60:6008–6017. [PubMed: 11085521]
27. Cunha, GR.; Donjacour, AA. Assessment of Current Concepts and Approaches to the Study of Prostate Cancer. New York: A.R. Liss; 1987. Mesenchymal-epithelial interactions: technical considerations; p. 273-282.
28. Yao V, Parwanai A, Maier C, Heston WD, Bacich DJ. Moderate expression of prostate-specific membrane antigen, a tissue differentiation antigen and folate hydrolase, facilitates prostate carcinogenesis. Cancer Res. 2008; 68:9070–9077. [PubMed: 18974153]
29. Bogel U, Dybdahl M, Frentz G, Nexo BA. DNA repair capacity: inconsistency between effect of over-expression of five NER genes and the correlation to mRNA levels in primary lymphocytes. Mutat Res. 2001; 461:197–210.
30. Friedberg EC. How nucleotide excision repair protects against cancer. Nat Rev. 2001; 1:22–33.
31. Varambally S, Yu J, Laxman B, Rhodes DR, Mehra R, Tomlins SA, Shah RB, Chandran U, Monzon FA, Becich MJ, Wei JT, Pienta KJ, Ghosh D, Rubin MA, Chinnaiyan AM. Integrative genomic and proteomic analysis of prostate cancer reveals signatures of metastatic progression. Cancer Cell. 2005; 8:393–406. [PubMed: 16286247]
32. Glinsky GV, Glinskii AB, Stephenson AJ, Hoffman RM, Gerald WL. Gene expression profiling predicts clinical outcome of prostate cancer. J Clin Invest. 2004; 113:913–923. [PubMed: 15067324]
33. Vanaja DK, Cheville JC, Iturria SJ, Young CY. Transcriptional silencing of zinc finger protein 185 identified by expression profiling is associated with prostate cancer progression. Cancer Res. 2003; 63:3877–3982. [PubMed: 12873976]

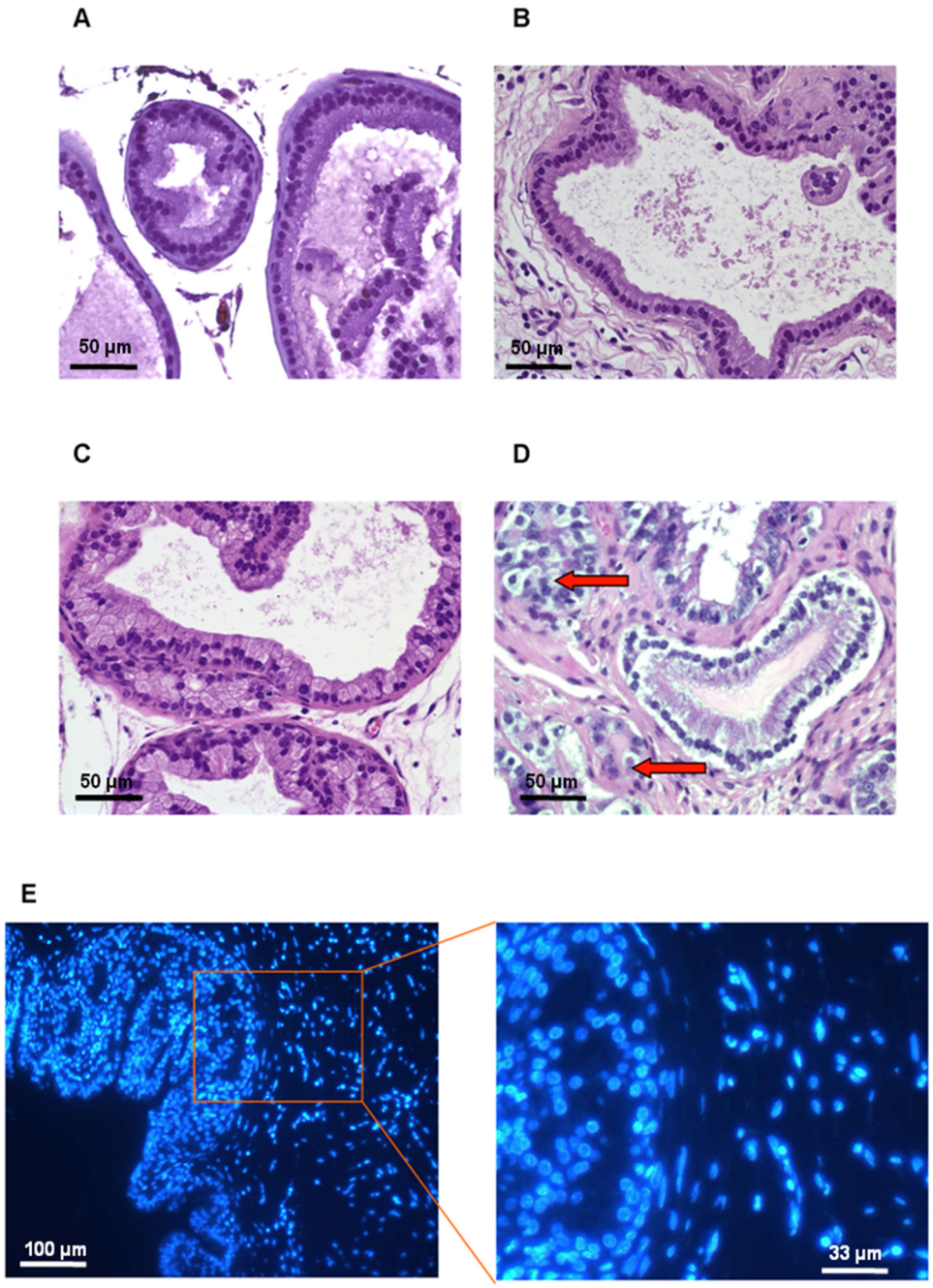

Figure 1.

Histological comparison of wild-type and *Ercc1*$^{-/-}$ tissue recombinants treated with T&E2 at 8 weeks post-renal grafting. (A) Prostate tissue from host Nude mouse. (B) Wild-type tissue recombinants displayed normal glandular architecture and focal hyperplasia. *Ercc1*$^{-/-}$ tissue recombinants displayed (C) 2+ PIN-like lesions, and (D) focal areas of nuclear pleomorphism, abnormal mitosis and crowding with epithelial proliferation. Arrows point to cells in mitoses. (A–D, scale bar = 50 μm) (E) Tissue sections were stained with Hoechst 33258 stain, with the nucleus of mouse origin having a spotty appearance while the cells of rat origin have a diffuse appearance. (left, scale bar = 100 μm; right, scale bar = 33 μm)

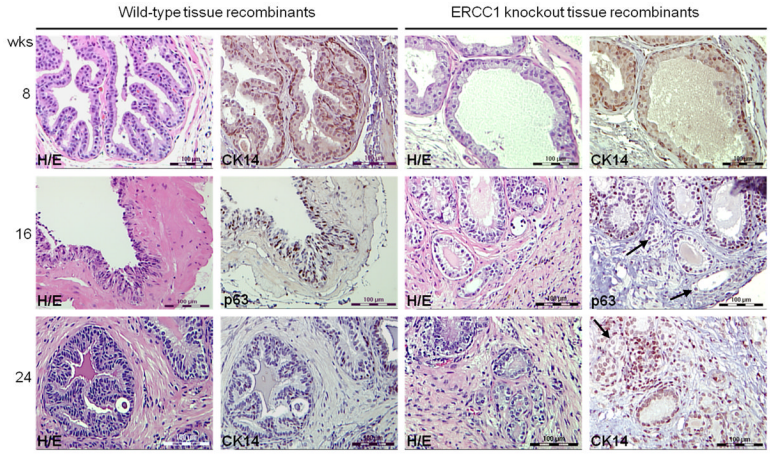

Figure 2.

Comparison of tissue recombinants at 8, 16 and 24 weeks post initial renal grafting. Small atypical glands with features of adenocarcinoma were observed only in *Ercc1*$^{-/-}$ tissue recombinants. H/E and CK-14/p63 staining of wild-type and *Ercc1*$^{-/-}$ tissue recombinants at 8, 16 and 24 weeks after renal grafting in immunodeficient hosts treated with T&E2. Arrows point to small atypical glands that lack of CK-14/p63-staining, indicative of adenocarcinoma (magnification ×20, scale bar = 100 μm).

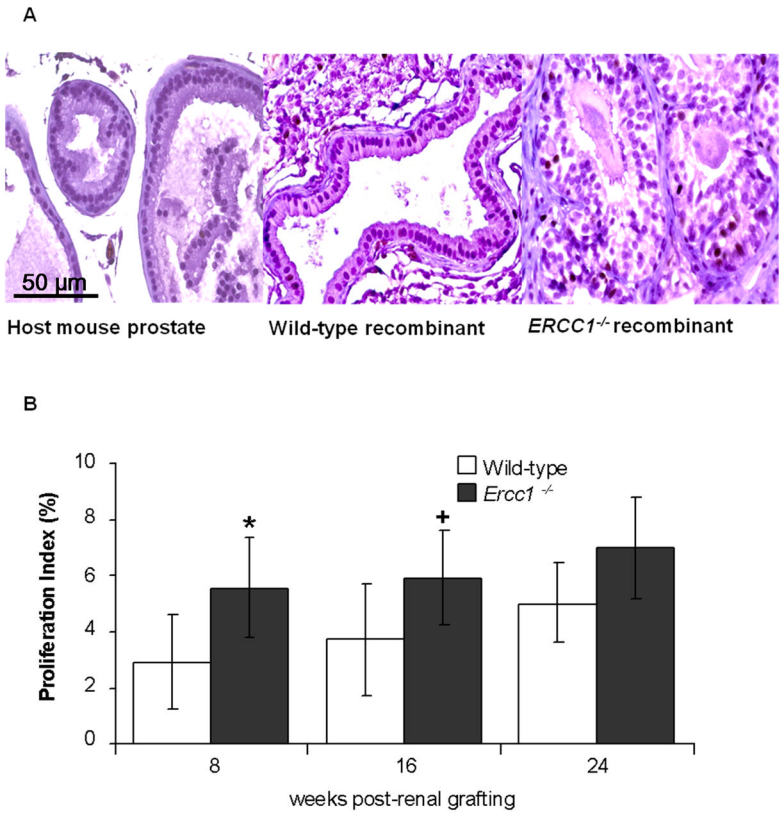

Figure 3.

Proliferation index of *Ercc1*$^{-/-}$ and wild-type tissue recombinants at 8 and 16 weeks post-renal grafting. (A) Histology of Ki67 stained host mouse prostate; wild-type, and *Ercc1*$^{-/-}$ prostate tissue recombinants at 16 weeks post-renal grafting (magnification ×20, scale bar = 50 μm). (B) Proliferation index of wild-type and *Ercc1*$^{-/-}$ tissue recombinants at 8, 16 and 24 post-renal grafting. Proliferation was significantly higher in Ercc1−/− tissue recombinants at 8 (*p=0.022) and 16 ($^{+}$p=0.033) weeks post-renal grafting. Data are presented as mean ± SEM.

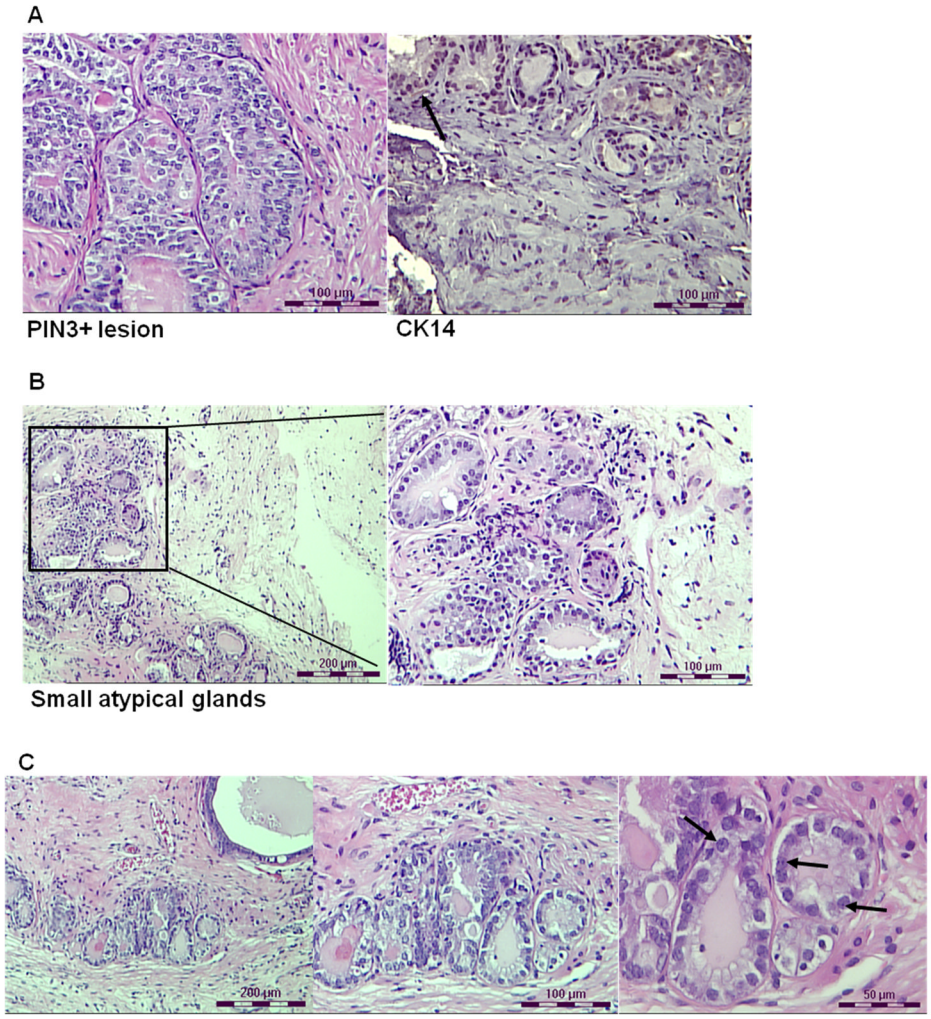

Figure 4.

Histology of *Ercc1*$^{-/-}$ tissue recombinants treated with T&E2 at 16 (A, B) and 24 (C) weeks post-renal grafting. (A) *Ercc1*$^{-/-}$ tissue recombinants displayed 3+ PIN-like lesion with hyperplasia, nuclear stratification, elevated nuclear to cytoplasmic ratios and papillary tufting and wisps of CK-14 positive (arrow) basal cells (scale bar = 100 μm; left and right panels are independent images). (B) Representative images of the same *Ercc1*$^{-/-}$ tissue recombinant with multiple, small, crowded glands with nuclear pleomorphism, elevated nuclear to cytoplasmic ratio, and abnormal mitosis – all characteristics indicative of carcinoma. (left, scale bar = 200 μm; right, scale bar = 100 μm) (C) Representative images of the same *Ercc1*$^{-/-}$ tissue recombinant at 24 weeks that displayed multiple small, crowded glands with large prominent nucleoli (arrows), high nuclear to cytoplasmic ratio, and abnormal mitosis (left, scale bar = 200 μm; middle, scale bar = 100 μm; right, scale bar = 50 μm).

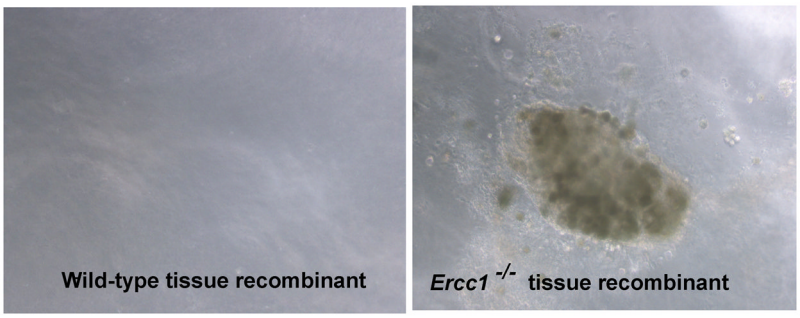

Figure 5.
Growth of cells from 24 week tissue recombinants in semisolid media. Cells isolated from wild-type tissue recombinants did not form colonies on semisolid medium. In contrast, cells isolated from *Ercc1*$^{-/-}$ tissue recombinants that had been grafted under the renal capsule for 24 weeks were able to form colonies on semisolid medium.

Table 1

Histopathology of prostatic epithelial cells in wild-type and *Ercc1*$^{-/-}$ tissue recombinants. The table depicts the most severe histopathological phenotype for each *Ercc1*$^{-/-}$ and wild-type tissue recombinant at 8, 16 and 24 weeks post-renal grafting. Only *Ercc1*$^{-/-}$ tissue recombinants displayed adenocarcinoma.

	Ercc1	(n)	Normal	Hyperplasia	PIN	Atypical glands with features of adenocarcinoma
8 week	+/+	11	2 (18%)	5 (46%)	4 (35%)	0 (0%)
	−/−	18	1 (5%)	3 (17%)	13 (72%)	1 (6%)*
16 week	+/+	15	1 (6%)	4 (27%)	10 (67%)	0 (0%)
	−/−	16	0 (0%)	0 (0%)	14 (87.5%)	2 (12.5%)$^{\#}$
24 week	+/+	13	4 (31%)	3 (23%)	6 (46%)	0 (0%)
	−/−	17	0 (0%)	0 (0%)	14 (82%)	3 (18%)$^{+}$

Statistical significance between *Ercc1*$^{-/-}$ and wild-type tissue recombinants were *p = 0.020, $^{\#}$p = 0.0065, and $^{+}$p = 0.0003 at the 8,16, and 24 week time points respectively. With serial grafting ERCC1−/− tissue recombinants progressed to a more severe histopathological phenotype more rapidly than wild-type (p=0.011).

Table 2

PIN-like lesions in wild-type and *Ercc1*$^{-/-}$ tissue recombinants were scored as 1+, 2+ or 3+ in cytological and architectural atypia. *Ercc1*$^{-/-}$, but not wild-type, tissue recombinants displayed 3+ PIN-like lesions at 8, 16 and 24 weeks post-renal grafting.

	Ercc1	**(n)**	**1+ PIN**	**2+ PIN**	**3+ PIN**
8 weeks	+/+	4	2 (50%)	2 (50%)	0 (0%)
	−/−	13	6 (46%)	5 (38%)	2 (15%)
16 weeks	+/+	10	5 (50%)	5 (50%)	0 (0%)
	−/−	14	4 (29%)	5 (36%)	5 (36%)
24 weeks	+/+	6	1 (17%)	5 (83%)	0 (0%)
	−/−	14	2 (14%)	9 (64%)	3 (21%)